



Published in final edited form as:

Hear Res. 2023 August ; 435: 108819. doi:10.1016/j.heares.2023.108819.

Development and evaluation of helper dependent adenoviral vectors for inner ear gene delivery

Osama Tarabichi¹, Tatiana Correa¹, Emre Kul², Stacia Phillips², Bahaa Darkazanly¹, Samuel M. Young Jr^{1,2,5,*}, Marlan R. Hansen^{1,3,4,5}

¹Departments of Otolaryngology-Head and Neck Surgery, University of Iowa, Iowa City, IA 52242

²Departments of Anatomy and Cell Biology, University of Iowa, Iowa City, IA 52242

³Departments of Neurosurgery, University of Iowa, Iowa City, IA 52242

⁴Departments of Molecular Physiology and Biophysics, University of Iowa, Iowa City, IA 52242

⁵Departments of Iowa Neuroscience Institute University of Iowa, Iowa City, IA 52242

Abstract

Viral vector gene therapy is an attractive strategy to treat hearing loss. Since hearing loss is due to a variety of pathogenic signaling cascades in distinct cells, viral vectors that can express large or multiple genes in a cell-type specific manner are needed. Helper-dependent adenoviral vectors (HdAd) are safe viral vectors with a large packaging capacity (~36 kb). Despite the potential of HdAd, its use in the inner ear is largely unexplored. Therefore, to evaluate the utility of HdAd for inner ear gene therapy, we created two HdAd vectors that use distinct cellular receptors for transduction: HdAd Serotype Type 5 (HdAd5), the Coxsackie-Adenovirus Receptor (CAR) and a chimeric HdAd 5/35, the human CD46+ receptor (hCD46). We delivered these vectors through the round window (RW) or scala media in CBA/J, C57Bl6/J and hCD46 transgenic mice. Immunostaining in conjunction with confocal microscopy of cochlear sections revealed multiple cell types were transduced using HdAd5 and HdAd 5/35 in all mouse models. Delivery of HdAd5 via RW in the C57Bl6/J or CBA/J cochlea resulted in transduced mesenchymal cells of the peri-lymphatic lining and modiolar region while scala media delivery resulted in transduction of supporting cells and inner hair cells. Hd5/35 transduction was CD46 dependent and RW delivery

* **Corresponding authors:** Samuel M. Young, Jr, PhD, Department of Anatomy and Cell Biology, University of Iowa, PBDB 5322, 169 Newton Road, Iowa City, IA 52242, samuel-m-young@uiowa.edu.

Author statement

Osama Tarabichi: Methodology, Formal Analysis, Investigation, Data Curation, Writing- Original draft Reviewing and Editing Validation Visualization funding acquisition

Tatiana Correa: Methodology, Formal Analysis, Investigation, Data Curation, Validation funding acquisition

Emre Kul: Methodology, Validation Writing- reviewing

Stacia Phillips: Methodology, Validation. Writing reviewing

Bahaa Darkazanly: Investigation, Formal Analysis

Samuel M. Young, Jr. : Conceptualization, Methodology, Verification, Project administration, Supervision, Validation, Writing – Original draft Reviewing and Editing funding acquisition

Marlan R. Hansen: Conceptualization, Methodology, Verification, Project administration. Supervision, Validation, Original draft Reviewing and Editing, funding acquisition

Publisher's Disclaimer: This is a PDF file of an unedited manuscript that has been accepted for publication. As a service to our customers we are providing this early version of the manuscript. The manuscript will undergo copyediting, typesetting, and review of the resulting proof before it is published in its final form. Please note that during the production process errors may be discovered which could affect the content, and all legal disclaimers that apply to the journal pertain.

of HdAd5/35 in the hCD46 mouse model resulted in a similar transduction pattern as HdAd5 in the peri-lymphatic lining and modiolar region in the cochlea. Our data indicate that HdAd vectors are promising vectors for use in inner ear gene therapy to treat some causes of hearing loss.

Keywords

Gene therapy; Helper dependent adenovirus; Inner ear; Hearing loss

1. Introduction:

Hearing loss impacts over 5% of the world population and has debilitating effects on communication which lead to increased rates of depression, anxiety, cognitive decline, and risk of dementia (1). Sensorineural hearing loss (SNHL) is the most common type of hearing loss that affects 466 million people worldwide (2). SNHL is due to loss or dysfunction of hair cells and spiral ganglion neurons, the two cell types essential for hearing (1). While our understanding of the genes and signaling cascades regulating the health and function of hair cells and spiral ganglion neurons continues to grow at an explosive pace (3), the ability to translate this knowledge into effective treatments for hearing loss lags far behind. To date, no FDA approved biological treatments exist to improve or restore auditory function. Hearing aids rehabilitate SNHL but do not restore cochlear function or stop hearing loss progression. Cochlear implants are the only way to restore hearing function in deaf patients, however they are limited in their ability to accurately transduce auditory information and are considered a last resort treatment (4). Therefore, there is an urgent need to develop novel biological therapeutics to overcome the limited treatment strategies available to address this growing health crisis.

Due to recent clinical successes of viral vector gene therapy, it is a promising therapeutic approach to treat SNHL (5). In contrast to other therapeutic strategies, viral vectors have the potential to treat SNHL with a single administration by stably expressing a transgene(s) that corrects the underlying cause (6), protects against further deterioration, or enhances neural survival (7). Currently, adeno-associated virus (AAV) is a leading candidate viral vector for inner ear gene therapy due to its low toxicity profile and ability to broadly transduce cells within the inner ear (8). Although AAV has tremendous potential for treating certain classes of SNHL, its small packaging capacity (~4.8kb) restricts its use in treating many causes of SNHL. Although dual AAV therapy approaches will express transgenes that exceed the AAV packaging limit, these approaches can lead to highly variable results due to low efficiency and truncated transcripts that can result in expression of dominant negative mutants (9).

Recombinant Adenoviral vectors (Ad) have packaging capacities that are up to 7 times greater than AAV packaging capacities and have had great success in basic research and clinical applications. Furthermore, 1st generation Ad vectors can transduce a wide variety of inner ear cell types and clinical trial results ([NCT02132130](#)) have demonstrated their safety in the human inner ear. Although early generation Ad vectors are considered safe, they can lead to ototoxicity due to expression of proteins from the remaining viral genome (10). Helper dependent adenoviral (HdAd) vectors are devoid of all viral genes and have

a large packaging capacity (~36 kb). HdAd vectors are safe, as preclinical trials with HdAd have demonstrated long-term correction in multiple mammalian disease models which include Duchenne muscular dystrophy, hyperbilirubinemia and Pompe's disease with a single administration of HdAd which was not possible with 1st generation Ad vectors (11–13).

Despite the tremendous potential of HdAd, its use in the inner ear has been largely unexplored. Therefore, we set out to characterize HdAd transduction in the inner ear using delivery through the round window (RW) or scala media to assess differences in transduction seen with delivery to the perilymphatic and endolymphatic compartments. To do so we created an HdAd5 vector which infects cells through the Coxsackie-Adenovirus Receptor (CAR) and a chimeric HdAd 5/35 vector that uses the hCD46 receptor to infect cells. Subsequently, we analyzed HdAd5 transduction patterns in the inner ear of neonatal C57Bl6J and adult CBA/J mice. In parallel, we analyzed HdAd5/35 transduction in the inner ear of CBA/J and hCD46 transgenic mice to study the impact of hCD46 on inner ear transduction patterns. We found that RW delivery of HdAd5 lead to transduction in mesenchymal cells of the peri-lymphatic lining and modiolar region while scala media delivery leads to transduction within the organ of Corti. We found that RW delivery of HdAd 5/35 transduces cells in a similar pattern to HdAd5 but in a hCD46 dependent manner. Based on these data, we find that RW delivery of HdAd5 or HdAd5/35 does not lead to transduction of organ of Corti cells but scala media delivery of HdAd5 does. Taken together, our data indicate that HdAd5 and HdAd5/35 vectors are promising vectors for use in inner ear gene therapy to treat hearing loss. However, further developments that improve the ability of HdAd vectors to transduce the organ of Corti via RW delivery are needed.

2. Methods:

2.1 Helper Viruses HV5 and HV5/35

HV5 was created from the adenovirus serotype 5 genomic helper virus plasmid pNG163-R2 (kind gift from Philip Ng, Baylor College of Medicine (14)) that was also used as the starting material to construct chimeric HV5/35. HV5/35 plasmid, named pNG163-R2–5T/35F, was created by excising the shaft and knob sequences of the fiber domain from pNG163-R2 and replacing those with serotype 35 shaft and knob sequences (Acc. no.: AY128640.2, bp:30961–31797). pNG163-R2 was digested with Cas9 nuclease from *S. Pyogenes* (NEB, Ipswich, MA, USA) using sgRNAs spanning the fiber domain with sequences 5'-gggactcttgaaccat-3' upstream and 5'-cttagtggttatccaca-3' downstream. The sgRNAs were synthesized using the EnGen sgRNA Synthesis Kit and purified using the Monarch RNA Clean Up Kit (NEB, Ipswich, MA, USA). The Cas9 reaction was treated with Proteinase K and heat inactivated. A synthetic DNA fragment harboring the serotype 35 shaft and knob and terminal 15 bp homology arms (Thermo Fisher Scientific, Waltham, MA, USA) was inserted using In-Fusion Cloning (TakaraBio, San Jose, CA, USA). Proper insertion and sequence integrity of the fragment was confirmed by Sanger sequencing. HV5 and HV5/35 viruses were produced according to the standard protocols (15) via transfection of PacI digested pNG163-R2 or pNG163-R2–5T/35F into a 6 cm dish of 293 cells and purified based on density by sequential centrifugation in cesium chloride.

The identities of purified helper viruses have been confirmed via PCR using a combination of forward primers specific to either serotype 5 fiber 5'-actggtctggccacaactac-3' or to serotype 35 fiber 5'-tgactagttatgatagaagtctatttccttg-3' and a common reverse primer 5'-gacaggaaccggtggaataaac-3'. The viral DNA from each helper virus was heat extracted at 95 °C for 10 mins, spin column purified (NucleoSpin-MachereyNagel, Dueren, Germany), and subjected to PCR amplification via standard Taq polymerase reaction (EconoTaq-Lucigen, Middleton, WI, USA). PCR products were visualized on a 1% agarose gel stained with ethidium bromide. The heat extracted viral DNA was used for the determination of physical titers via spectrophotometry measuring absorbance at 260 nm. The titer (vp/mL) was calculated as follows: $\text{vp/mL} = (A_{260} \times \text{dilution factor} \times 1.1 \times 10^{12} \times 36) / \text{vector genome size in kb}$ (19).

2.2 HdAd5 and HdAd5/35 Vectors

Two transgene expression cassettes consisted of either CMV or CAG promoters together with the green fluorescent reporter protein mClover3, chimeric intron, and simian virus polyadenylation signal (SV40polyA) sequences were constructed in shuttle plasmids via restriction cloning. The cassettes were then transferred to the HdAd plasmid C4HSU (14) via In-Fusion cloning (TakaraBio, San Jose, CA, USA) to yield pHdAd CMV mClover3 and pHdAd CAG mClover3. Each HdAd plasmid was PmeI digested and transfected into a 6 cm dish of 116 cells. Twenty-four hours later, the dishes were infected with either HV5 or HV5/35 to generate HdAd5 or HdAd5/35 respectively. Cells were harvested when they exhibited full cytopathic effect. Following standard protocols (15, 16), a total of four serial amplifications was performed for HdAd5 vectors with the final passage harvested from thirty 15 cm dishes. HdAd5/35 vector was amplified in six passages in 116 cells. Finally, the HdAd5 CMV mClover3 (concentration: 2.29×10^{12} vp/ml), HdAd5 CAG mClover3 (concentration: 2.55×10^{12} vp/ml), and HdAd5/35 CAG mClover3 (concentration: 8.07×10^{11} vp/ml) vectors were CsCl density gradient purified, dialyzed against a biocompatible storage buffer (10 mM HEPES, 250 mM sucrose, 1 mM MgCl₂ at pH 7.4), and stored at -80 °C for subsequent *in vivo* injections. Physical titers were determined as described for helper viruses.

2.3 Animals

All animal procedures were approved by the University of Iowa institutional animal care and use committee (Protocol # 0122081). Three separate animal models were used to characterize viral vector transduction: 1) 8–12 week old CBA/CaJ adult mice. 2) Neonatal P4–5 C57/Bl6J mice and 3) 8–12 week old Human CD46 transgenic mice on C57/Bl6J background. The hCD46 transgenic model (Jackson Laboratory) carries a YAC-CD46 transgene that codes for the complement regulatory protein CD46 under direction of the human CD46 promoter(17). The hCD46 mouse genotype was verified by polymerase chain reaction using standard protocol from Jax.

2.4 Surgical procedures

Three surgical approaches were used to fully characterize vector transduction. RW approach was used in neonatal C57/Bl6J mice. RW with posterior semicircular canal fenestrations

(RW+CF) approach was used in adult CBA/CaJ mice and hCD46 transgenic mice. Scala media approach was performed in adult CBA/CaJ mice.

2.4.1 Round window approach in neonatal mice—Neonatal mice were anesthetized using hypothermia. To achieve this, neonatal pups were wrapped in a latex glove and submerged up to the neck in crushed ice and water for about 5–8 minutes and adequate depth of anesthesia was confirmed by lack of spontaneous movement or pedal withdrawal to a toe pinch with a micro forceps. A post-auricular incision and dissection of underlying subcutaneous tissue and muscle to expose the otic bulla was performed. Bullostomy was then created with sharp dissection using micro scissors and the round window is identified. Glass pipette loaded with the vector and housed in a micromanipulator is then used to penetrate the round window and 1 μ l of HdAd5-CAG-mclover3 (2.55×10^9 viral particles per animal) vector is injected into the scala tympani. A muscle plug and vetbond tissue adhesive are then used to seal the round window. The wound is then closed with 6–0 prolene sutures in an interrupted fashion. Pups are then returned to their mother's cage placed over a warming pad for recovery. Mice are monitored daily for adequate recovery for 5 days postoperatively

2.4.2 Round window and posterior canal fenestration approach in adult mice—RW with posterior semicircular canal fenestration (RW+CF) approach was performed as described by Yoshimura et al(18). Anesthesia is induced using a mixture of 100 mg/kg xylazine and 10 mg/kg of yklazine. Depth of anesthesia is monitored using pedal withdrawal to toe pinch. A post-auricular incision is made and dissection of subcutaneous tissue and muscle is performed to expose the underlying otic bulla. A drill is used to create a bullostomy which is widened until the round window and stapedia artery are adequately visualized. Further dissection is then carried out to expose the posterior semicircular canal and a small canalostomy is performed. Completion of canalostomy is confirmed by visualizing slow egress of peri-lymphatic fluid. Glass pipette loaded with the vector and housed in a micromanipulator is then used to penetrate the round window and 1.5 μ l of HdAd5-CAG-mclover3 (3.83×10^9 viral particles/animal), HdAd5-CMV-mclover3 (3.44×10^9 viral particles/animal) or HdAd5/35-CAG-mclover3 (1.21×10^9 viral particles/animal) vector is injected into the scala tympani. A muscle plug and vetbond tissue adhesive are then used to seal the round window and canal fenestration. The incision is then closed using 6–0 prolene sutures in an interrupted fashion. Mice were then placed back in their cage with a warming pad underneath for recovery. Mice are monitored daily for adequate recovery for 5 days postoperatively.

2.4.3 Scala media injection—Mice are anesthetized in a similar fashion to RW+CF approach. Post-auricular incision and bullostomy are performed similar to RW+CF approach. Bullostomy is widened until the round window, stapedia artery and basal turn of the cochlea could be visualized. A small cochleostomy is gently performed in the basal turn and 1.5 μ l HdAd5-CMV-mclover3 (3.44×10^9 viral particles/animal) vector solution is delivered directly into the scala media. A muscle plug and vetbond tissue adhesive (3M, St Paul, MN, USA) are then used to seal the cochleostomy. Incisions were closed using 6–0 prolene sutures (Ethicon, Raritan, NJ, USA). Mice were then placed back in their cage with

a warming pad underneath for recovery. Mice are monitored daily for adequate recovery for 5 days postoperatively.

2.5 Histologic preparation

All mice were euthanized at a seven-day time point after viral vector delivery. Euthanasia was performed by decapitation in neonatal mice and 100% CO₂ administration for adult mice. Cochleae were immediately extracted following euthanasia and fixed in 4% paraformaldehyde solution for 4–16 hours, rinsed, and stored in PBS. Cochleae were prepared using both whole mount organ of Corti preparations and mid-modiolar cryo-sections. For whole mount preparations, cochleae were micro dissected in PBS to extract apical and basal segments of the organ of Corti. Dissected samples were permeabilized and blocked using 0.1% Triton X-100 and 5% goat serum for 1 hour at room temperature. Samples were then incubated in rabbit polyclonal anti-myosin VIIa antibody (1:200 dilution of 1 mg/ml antibody solution; Proteus biosciences, Ramona, CA, USA) and mouse monoclonal anti-NF200 (1:200 dilution of 2 mg/ml antibody solution; Sigma-Aldrich, St. Louis, MO, USA) antibody solution at 4 C overnight. Following primary antibody incubation samples were washed in PBS and incubated in goat anti-rabbit AlexaFluor 546 (1:400 dilution of 2 mg/ml antibody solution; Thermo Fisher Scientific, Waltham, MA, USA), goat anti-mouse AlexaFluor 647 (1:400 dilution of 2 mg/ml antibody solution; Thermo Fisher Scientific, Waltham, MA, USA) and DAPI (1:1,000 of 1 mg/ml solution; Thermo Fisher Scientific, Waltham, MA, USA) for 1 hour at room temperature. Following secondary antibody incubation samples were mounted on to glass slides with Fluoromount-G (Southern Biotech, Birmingham, AL, USA) mounting media. For mid-modiolar sectioning preparations cochleae were decalcified in 0.1M ethylene-diaminene-tetra-acetic acid (EDTA) for 72–96 hours following fixation in PBS. Cochleae were then cryopreserved by incubation in serial dilutions of sucrose solution (10% sucrose for 24 hours followed by 30% sucrose solution for 24 hours) and then embedded in OCT medium and frozen. 10 um frozen sections were acquired. Blocking, permeabilization and antibody incubations were performed in a similar manner to whole mounts.

2.7 Image Analysis

Confocal microscopy was performed using a Stellaris 5 confocal microscope (Leica microsystems, Wetzlar, Germany). Initial scout images were obtained using a 10x objective. 63x immersion objective was used to obtain images used for quantitative analysis. 405 diode laser and white light laser were used for excitation of fluorophores. 405 diode laser was used to excite the DAPI signal. White light laser with spectral range spanning from 485 to 790 nm was used to excite remaining fluorophores which included mClover3 (488 nm) signal, AlexaFluor 546 signal (myosin7a) and AlexaFluor 647 signal (NF-200). Z-stack images were performed on whole mount and mid-modiolar section samples. Z-stack step-size was 0.36 microns and slice thickness was 0.72 microns for images obtained under 63x objective. Image stacks were then analyzed in Imaris cell imaging software (Oxford instruments, Abingdon, United Kingdom). 3-D volumetric reconstructions of z-stack images were created on the Imaris platform. Volumetric reconstructions were segmented in to two different anatomical subregions: 1) The basilar membrane region underlying the organ of Corti and 2) the modiolar region. Total cell counts in each of the regions was performed by determining

the total number of nuclei stained using an automatic counting function that detects discrete DAPI stained objects with a set diameter of approximately 5–10 microns in diameter (average diameter of a cellular nucleus)(19). Transduced cell counts were then obtained by selecting nuclei that colocalized to the mClover3 signal. Transduction efficiencies were reported as percentage of total cells transduced per anatomical subregion.

2.7 Statistical analysis

Descriptive statistics for viral transduction efficiency are described below and tabulated in figures. Results were analyzed using two-tailed t tests with assumption of unequal variance and with a significance level of $\alpha=0.05$.

3. Results

3.1 HdAd5 delivered by RW+CF transduces mesenchymal cells lining basilar membrane and in the modiolus in adult CBA/CaJ mice.

Previous results demonstrated that delivery of AdType5 and AAV via the RW transduction was largely restricted to in the base of the cochlea (20, 21). However, recent work has shown that the RW+CF approach with AAV leads to widespread transduction from base to apex in the cochlea (18). Therefore, we set out to evaluate HdAd transduction in the mouse inner ear at different developmental time points (Figure 1). First to determine if the RW+CF approach enabled HdAd transduction throughout the cochlea we delivered HdAd5 CMV mClover3 using the RW+CF approach in adult CBA/CaJ mice. Analysis of the cochlea 7 days later revealed that RW+CF leads to widespread transduction from base to apex in the cochlea and in an average of 34.2% of cells in the apical region and 34.8% of cells in the basal region (n=4 CBA/CaJ mice, age 8–12 weeks) (Figure 2 A,B). We found that transduction was limited to mesenchymal cells lining the basilar membrane and there was very minimal transduction in the modiolar region (Figure 2 A,B). Close inspection in the modiolar region revealed that transduction was limited to non-neuronal transduction and no transduction was detected in the organ of Corti.

To determine if our transduction results seen were due to HdAd5 tropism or due to the CMV promoter, we developed an HdAd5-CAG-mClover3 to evaluate if the CAG promoter resulted in different transduction patterns. Using the RW+CF approach, we found that HdAd5-CAG-mClover3 transduced 29.67% of basilar membrane cells in the apical region and 9.54% of cells in the basal region (n=5 CBA/CaJ mice, age 8–12 weeks) (Figure 2 C,D,E,F). Analysis of transduction in the modiolus regions reveal that 7.61% of cells in the apical region and 7.64% of cells in the basal region of the modiolus were transduced. However, no cells in the organ of Corti were transduced. Although both vectors lead to basilar membrane transduction, HdAd5-CAG-mClover3 led to a distinct base to apex transduction pattern compared to HdAd CMV-mClover3 (Fig 1H). There was no significant quantitative difference in either apical ($p=0.67$) or basal transduction ($p=0.08$) of mesenchymal cells lining the basilar membrane. In addition, HdAd5 CAG-mClover3 led to transduction of modiolar cells when compared to HdAd5-CMV-mClover3 which showed little to no transduction of modiolar cells. Taken together, these results demonstrate that HdAd5 delivery with RW+CF leads to transduction throughout the cochlea that, regardless

of promoter used, is restricted to the basilar membrane and non-neuronal cells in the modiolar region with no transduction in the organ of Corti.

3.2 HdAd5 delivered by scala media approach transduces supporting cells in the organ of Corti and inner hair cells in adult CBA/CaJ mice.

The apical side of the cells in the organ of Corti are directly accessible via the scala media, while the basal side of cells in the organ of Corti are accessible with RW delivery. Therefore to evaluate if the route of delivery was a key determinant in transduction patterns and if HdAd5 could transduce cells in the organ of Corti, we delivered HdAd5-CMV-mClover3 into the organ of Corti through the scala media by performing a cochleostomy (n=4 CBA/CaJ mice, age 8–12 weeks) (Figure 3). Subsequently, seven days after delivery we found that the scala media approach led to transduction in the organ of Corti with supporting cells as the dominant cell type transduced with some inner hair cell transduction. Based on anatomic location of the transduced cells, they were identified to be Deiters cells, inner pillar cells and outer pillar cells. Additionally, transduction was seen in the modiolus and transduction restricted to mesenchymal cells and no neuronal transduction was seen. Despite the ability to transduce cells in the organ of Corti, this approach was destructive and led to widespread loss of outer hair cells. Based on our data, we conclude that the route of delivery is the primary determinant of inner ear transduction patterns and that HdAd5 vectors can transduce cells in the organ of Corti.

3.3 HdAd5 delivered by RW alone in neonatal C57/Bl6 mice transduces mesenchymal cells lining the basilar membrane and modiolus.

AAV vector transduction patterns in the inner ear at different developmental time points between neonatal and adult mice are different (22). Therefore, we wanted to determine if the developmental state of the inner ear impacted HdAd transduction patterns. CAR receptor expression is highly expressed at most cell-types in the inner ear of P1-P6 mice including inner and outer hair cells (23). However, in the adult mouse cochlea it is restricted to pillar cells and cell-cell junctions in the stria vascularis (23). Therefore, to determine if HdAd5 could transduce cells in the neonatal cochlea, we delivered HdAd5-CAG-mClover3 in neonatal C57/Bl6 using an RW approach without CF. RW+CF was not done due the size of neonatal pups. Analysis of cochlear tissues seven days after injection showed that cells were transduced in a similar pattern to that seen with adult mice. In the basilar membrane, HdAd5-CAG-mClover3 transduced 12.86% of cells in the apical region and 12.05% of cells in the basal region (n=5 neonatal C57/Bl6 mice, age P4–5) (Figure 4) with no significant difference in transduction efficiency when compared to adult mice in both the apical (p=0.09) and basal regions (p=0.61). In the modiolar region, we found 7.37% of cells in the apical region and 11.09% in the basal region were transduced with no significant difference in transduction efficiency when compared to adult mice in both the apical (p=0.87) and basal (p=0.44) regions. Therefore, we conclude that the increased CAR expression reported in the neonatal mouse cochlea does not lead to increased HdAd5 transduction.

3.4 HdAd5/35 leads to similar transduction patterns as HdAd5 but leads to higher levels of transduction in the inner ear of a hCD46 transgenic mouse.

A determinant of viral vector tropism is the primary attachment receptor. There are several classes of Ad viral groups that use distinct primary attachment receptors for receptors and transduce cells in a CAR independent manner. In contrast to Group C Ad viruses which use CAR, Group B Ad virus use the CD46 receptor as their primary attachment receptor (24). While the hCD46 receptor binding properties and expression patterns are distinct from the mouse CD46 receptor, a human CD46 transgenic mouse line exists. Although every nucleated cell in this mouse line expresses CD46, whether cells in the cochlea of these mice express hCD46 was unknown. Therefore, hCD46 expression in the cochlea was confirmed by immunolabelling and confocal microscopy. (Figure 5). We found that CD46 was expressed on the surface of multiple cell types within the cochlea including inner and outer hair cells, organ of Corti supporting cells and widespread transduction in the basilar membrane lining.

Ad Type 35 and Ad5/35 chimeras have been successfully shown to transduce CAR negative but CD46 positive cells. Therefore, we created a HdAd5/35 chimera (HdAd5/35-CAG-mClover3) and delivered this vector via RW+CF approach in both adult CBA/CaJ $n=4$ CBA/CaJ mice, age 8–12 weeks) and CD46 transgenic mice ($n=3$ hCD46 transgenic mice, Age 8–12 weeks). In CBA/CaJ mice HdAd 5/35-CAG-mClover3 showed minimal transduction overall, with only 1.54 and 2.60% of cells in the basilar membrane region of the apical and basal segments transduced respectively. Two out of four cochleae in the CBA/CaJ analyzed showed transduction in modiolar regions only with no transduction in the basilar membrane regions throughout the cochlea. HdAd5/35-CAG-mClover3 transduced 3.18% and 1.58% of cells in the modiolar region of the apical and basal segments respectively. In contrast, in the hCD46 transgenic mice HdAd5/35 resulted in significant transduction in both the basilar membrane and modiolar region. In the basilar membrane region, 45.10% and 43.03% of cells in the apical and basal regions were transduced (Figure 6). In the modiolar region 8.31% and 13.21% of cells in apical and basal regions were transduced. Transduction in the apical region was significantly higher in hCD46 mice when compared to wild type CBA/CAJ mice for both mesenchymal cells in the basilar membrane ($p=0.03$) and modiolar cells ($p=0.01$). Transduction of these regions in the base was noted to be higher on average in hCD46 mice but differences were not statistically significant based on a significance level of 0.05. Based on these results, we demonstrate that HdAd5/35 transduces the inner ear in a CD46 dependent manner that was restricted to mesenchymal cells in the basilar membrane and non-neuronal cells in the modiolar region with no transduction of the organ of Corti. Therefore, we conclude that HdAd5/35 does not lead to improved transduction or increased cell-type transduction in the cochlea of the hCD46 mouse model via RW delivery. No sex differences were noted in the patterns of transduction for each of the viral vectors and delivery routes. Quantitative analysis of transduction efficiency by mouse sex was not performed due to small group sizes.

4. Discussion

The large packaging capacity of HdAd vectors make them promising candidates for inner ear gene therapy as they overcome the packaging limitations of AAV and lentiviral vectors. In this study we evaluated the transduction patterns of two HdAd vectors that use different primary attachment receptors and the impact of different routes of administration in the inner ear of mice. We found that HdAd5 and HdAd5/35 vectors delivered into the perilymphatic space with the RW+CF or RW approach transduce mesenchymal cells lining the basilar membrane and modiolar region but did not transduce cells in the organ of Corti. Using delivery through the scala media, we found that HdAd5 broadly transduced supporting cells in the organ of Corti. Therefore, these results point that route of delivery is the major determinant of HdAd vector ability to transduce cells in the organ of Corti.

4.1 HdAd5 transduction patterns vary by route of delivery

Our results demonstrate the delivery of HdAd5 to perilymphatic space using clinically translatable routes of administration, RW or RW+CF, did not lead to transduction in the organ of Corti. However, delivery of HdAd5 directly to the scala media which provides direct access to the apical surface of cells in the organ of Corti resulted in transduction of multiple cell types within the organ of Corti. Although CAR is expressed in mesenchymal cells and the organ of Corti (25) our results suggest that the lack of transduction in the organ of Corti via RW delivery maybe due to the basilar membrane acting as anatomic barrier or inaccessibility of CAR in the organ of Corti. However, it has been reported that a 2nd generation Ad5 vector (26) delivered into the perilymphatic space lead to 99% and 97% transduction of inner and outer hair cells in the basal cochlea and 90% and 51% of inner and outer hair cells respectively in the apical section of the cochlea. In addition, transduction of mesenchymal cells appeared to be less robust. These results are in stark contrast to our findings and other reports using Ad5 delivery via the RW in rodents (25, 27). It is possible that the difference of results is due to multiple reasons including: 1) Potential species differences in CAR expression patterns in guinea pig vs mouse. This seems less likely as our findings are in line with Ishimoto et al.(27), who also used a guinea pig model or 2) The 50-fold difference in vector load delivered in the Luebke study (5×10^8 TU) (26) vs the Ishimoto study (1×10^7 TU) (27). The adenoviral VP:TU typically ranges anywhere from 100:1 to 30:1, therefore our vector dosages which were $1-3 \times 10^9$ VP correspond to a range of $\sim 1 \times 10^7$ to $\sim 1 \times 10^8$ TU and are similar to the those used by Ishimoto et al (27) and Luebke et al (26). Previous results have demonstrated that viral titers are a key determinant of transduction (28). Since there was a 50-fold difference in vector load, the disparity in viral vector load could be the key difference. In this scenario, mesenchymal cells of the perilymphatic lining could act as a “sponge” that uptakes the bulk of the viral particles and only leaves few vector particles to effectively traverse the basilar membrane and transduce cells in the organ of Corti. Therefore, future studies with increasing total amounts of HdAd5 will need to be performed to determine if the basilar membrane acts as a “sponge”.

In contrast to the RW delivery approach, delivery via scala media allows for direct access to the organ of Corti. Studies in comparable rodent models (rat) show widespread CAR expression throughout the organ of Corti (25) and that the CAR receptor appears to be

highly localized at the apical surface of hair cells and supporting cells with low levels at the basal membrane of hair cells and supporting cells. Our results are in line with previous reports of successful transduction of the organ of Corti in Ad5 mouse models (29–31). Therefore, these results suggest that organ of Corti transduction by HdAd5 using the scala media approach in the rodent model provides unimpeded access to CAR receptors that reside on the apical surface and are bathed by endolymph in the scala media. Despite the ability to transduce cells in the organ of Corti through scala media delivery, this approach results in damage to the hair cells. Therefore, this approach is not viable for hearing impaired individuals with residual hearing function.

While the inability to transduce the organ of Corti with HdAd 5 or HdAd5/35 delivery in to the perilymphatic compartment represents a major limitation of HdAd5 that needs to be solved, there are forms of hearing loss that represent good targets for HdAd based gene therapies. Adenoviral transduction of mesenchymal cells lining the scala tympani with neurotrophic factors such as GDNF has been shown to increase otoprotection after aminoglycoside mediated cochlear injury (32, 33). In addition, scala media delivery and transduction of supporting cells by HdAd to overexpress specific transcription factors could be used in hair cell regeneration gene therapy strategies (30).

4.2 Promoter choice and use of neonatal mouse model did not significantly impact transduction patterns of HdAd5

Promoters play a critical role in determining transduction profiles of viral vectors and can be used to determine rate limiting steps of viral vector transduction. Previous data from AAV based gene delivery suggest that a CAG promoter may improve transduction efficiency in hair cells, supporting cells and spiral ganglion cells (28) We found that transduction patterns in adult mice were roughly the same with CAG or CMV driven expression vectors with a potential increase in modiolar transduction with the CMV promoter. In addition, we found that injecting CAG vector into a P4–5 neonatal mice using a RW approach did not lead to transduction in the organ of Corti and showed similar transduction patterns to those seen in adult mice. Therefore, our data suggest that the CMV promoter was not the key determinant of Ad5 transduction but rather viral uptake into organ of Corti is the rate limiting step.

4.3 HdAd 5/35 CD46 mediated transduction patterns are similar to HdAd5

Since viral vector tropism is heavily determined by the primary attachment receptor, a plethora of research has gone into developing Ad vectors that exploit the natural diversity of Ad serotype tropism to transduce cells in a CAR independent manner (34–36). CD46 is ubiquitously expressed in humans, but expression has been seen to be limited to only testicular tissue in mice (37). The CD46 receptor is expressed on every nucleated cell and is the primary attachment receptor of Group B adenoviruses. Importantly, hCD46 transgenic mice are vulnerable to measles infections and HdAd5/35 chimera vector can transduce hematopoietic stem cells in the hCD46 mouse line (34, 36). Therefore, the hCD46 mouse line is well-suited to evaluate viral vectors targeting the hCD46 receptor. Our results demonstrated that HdAd5/35 transduction was determined by hCD46 expression. For example, we found that with RW+CF approach the overall pattern of transduction was similar to HdAd5, but there appeared to be increased overall transduction in the hCD46

model. Although immunostaining demonstrated that CD46 is highly expressed in the organ of Corti, and throughout inner and outer hair cells, we were unable to determine precise localization of the CD46 receptor. Therefore, it is possible that CD46 is not localized to the basilar membrane of the organ of Corti. However, it is also possible that high levels of CD46 expression in the basilar membrane prevent HdAd5/35 from reaching the organ of Corti. Therefore, future experiments will be needed to test these hypotheses. Since scala media injection is highly destructive we did not explore HdAd5/35 transduction efficacy following a scala media injection.

5. Conclusion:

Taken together our results show that HdAd vectors transduce a variety of cell types within the inner ear but are largely restricted from entering the organ of Corti when delivered to the scala tympani. Efforts to enhance transduction efficiency of HdAd5 did not lead to organ of Corti transduction in our model. CD46 mediated transduction of HdAd5/35 produced a similar pattern to HdAd5 transduction. Further studies on chimeric vectors using other Ad serotypes or other modified Ad vectors are warranted to increase our understanding of the parameters that dictate HdAd transduction in the inner ear.

Acknowledgments:

This work was supported by the following funding sources: NIDCD R21 DC018242 to SMY and MH. NIDCD T32 DC000040, NIDCD R01DC018488 and NIDCD R01DC012578 MH. R01 DC014093, R01 NS110742, R03TR004161 SMY. American Society of Pediatric Otolaryngology CORE research grant 2021–2022 OT. American Neurotology Society 2020 research grant TC.

References

1. Ahmed H, Shubina-Oleinik O, Holt JR. Emerging Gene Therapies for Genetic Hearing Loss. *J Assoc Res Otolaryngol* 2017.
2. Olusanya BO, Davis AC, Hoffman HJ. Hearing loss: rising prevalence and impact. *Bull World Health Organ* 2019;97(10):646–a. [PubMed: 31656325]
3. Dabdoub A, Fritzsich B, Popper AN, Fay RR, SpringerLink (Online service). The Primary Auditory Neurons of the Mammalian Cochlea Available from: 10.1007/978-1-4939-3031-9.
4. Mowry SE, Woodson E, Gantz BJ. New frontiers in cochlear implantation: acoustic plus electric hearing, hearing preservation, and more. *Otolaryngol Clin North Am* 2012;45(1):187–203. [PubMed: 22115690]
5. Atkinson PJ, Wise AK, Flynn BO, Nayagam BA, Richardson RT. Viability of long-term gene therapy in the cochlea. *Sci Rep* 2014;4:4733. [PubMed: 24751795]
6. Akil O, Seal RP, Burke K, Wang C, Alemi A, During M, et al. Restoration of hearing in the VGLUT3 knockout mouse using virally mediated gene therapy. *Neuron* 2012;75(2):283–93. [PubMed: 22841313]
7. Hashimoto K, Hickman TT, Suzuki J, Ji L, Kohrman DC, Corfas G, et al. Protection from noise-induced cochlear synaptopathy by virally mediated overexpression of NT3. *Sci Rep* 2019;9(1):15362. [PubMed: 31653916]
8. Sacheli R, Delacroix L, Vandenaekerveken P, Nguyen L, Malgrange B. Gene transfer in inner ear cells: a challenging race. *Gene Ther* 2013;20(3):237–47. [PubMed: 22739386]
9. McClements ME, MacLaren RE. Adeno-associated Virus (AAV) Dual Vector Strategies for Gene Therapy Encoding Large Transgenes. *Yale J Biol Med* 2017;90(4):611–23. [PubMed: 29259525]

10. Kügler S, Kilic E, Bähr M. Human synapsin 1 gene promoter confers highly neuron-specific long-term transgene expression from an adenoviral vector in the adult rat brain depending on the transduced area. *Gene Ther* 2003;10(4):337–47. [PubMed: 12595892]
11. Rastall DP, Seregin SS, Aldhamen YA, Kaiser LM, Mullins C, Liou A, et al. Long-term, high-level hepatic secretion of acid α -glucosidase for Pompe disease achieved in non-human primates using helper-dependent adenovirus. *Gene Ther* 2016;23(10):743–52. [PubMed: 27367841]
12. Gilbert R, Dudley RW, Liu AB, Petrof BJ, Nalbantoglu J, Karpati G. Prolonged dystrophin expression and functional correction of mdx mouse muscle following gene transfer with a helper-dependent (guttled) adenovirus-encoding murine dystrophin. *Hum Mol Genet* 2003;12(11):1287–99. [PubMed: 12761044]
13. Schmitt F, Pastore N, Abarrategui-Pontes C, Flageul M, Myara A, Laplanche S, et al. Correction of hyperbilirubinemia in gunn rats by surgical delivery of low doses of helper-dependent adenoviral vectors. *Hum Gene Ther Methods* 2014;25(3):181–6. [PubMed: 24593043]
14. Sandig V, Youil R, Bett AJ, Franlin LL, Oshima M, Maione D, et al. Optimization of the helper-dependent adenovirus system for production and potency in vivo. *Proc Natl Acad Sci U S A* 2000;97(3):1002–7. [PubMed: 10655474]
15. Montesinos MS, Satterfield R, Young SM Jr. Helper-Dependent Adenoviral Vectors and Their Use for Neuroscience Applications. *Methods Mol Biol* 2016;1474:73–90. [PubMed: 27515075]
16. Palmer DJ, Ng P. Rescue, amplification, and large-scale production of helper-dependent adenoviral vectors. *Cold Spring Harb Protoc* 2011;2011(7):857–66. [PubMed: 21724821]
17. Yannoutsos N, Ijzermans JN, Harkes C, Bonthuis F, Zhou CY, White D, et al. A membrane cofactor protein transgenic mouse model for the study of discordant xenograft rejection. *Genes Cells* 1996;1(4):409–19. [PubMed: 9135084]
18. Yoshimura H, Shibata SB, Ranum PT, Smith RJH. Enhanced viral-mediated cochlear gene delivery in adult mice by combining canal fenestration with round window membrane inoculation. *Sci Rep* 2018;8(1):2980. [PubMed: 29445157]
19. Li G-W, Xie XS. Central dogma at the single-molecule level in living cells. *Nature* 2011;475(7356):308–15. [PubMed: 21776076]
20. Chien WW, McDougald DS, Roy S, Fitzgerald TS, Cunningham LL. Cochlear gene transfer mediated by adeno-associated virus: Comparison of two surgical approaches. *Laryngoscope* 2015;125(11):2557–64. [PubMed: 25891801]
21. Staecker H, Li D, O'Malley BW Jr., Van De Water TR. Gene expression in the mammalian cochlea: a study of multiple vector systems. *Acta Otolaryngol* 2001;121(2):157–63. [PubMed: 11349769]
22. Bankoti K, Generotti C, Hwa T, Wang L, O'Malley BW Jr., Li D. Advances and challenges in adeno-associated viral inner-ear gene therapy for sensorineural hearing loss. *Mol Ther Methods Clin Dev* 2021;21:209–36. [PubMed: 33850952]
23. Excoffon KJ, Avenarius MR, Hansen MR, Kimberling WJ, Najmabadi H, Smith RJ, et al. The Coxsackievirus and Adenovirus Receptor: a new adhesion protein in cochlear development. *Hear Res* 2006;215(1–2):1–9. [PubMed: 16678988]
24. Gaggar A, Shayakhmetov DM, Lieber A. CD46 is a cellular receptor for group B adenoviruses. *Nature Medicine* 2003;9(11):1408–12.
25. Venail F, Wang J, Ruel J, Ballana E, Rebillard G, Eybalin M, et al. Coxsackie adenovirus receptor and alpha nu beta3/alpha nu beta5 integrins in adenovirus gene transfer of rat cochlea. *Gene Ther* 2007;14(1):30–7. [PubMed: 16886000]
26. Luebke AE, Foster PK, Muller CD, Peel AL. Cochlear function and transgene expression in the guinea pig cochlea, using adenovirus- and adeno-associated virus-directed gene transfer. *Hum Gene Ther* 2001;12(7):773–81. [PubMed: 11339894]
27. Ishimoto S, Kawamoto K, Kanzaki S, Raphael Y. Gene transfer into supporting cells of the organ of Corti. *Hear Res* 2002;173(1–2):187–97. [PubMed: 12372646]
28. Verdoodt D, Peeleman N, Van Camp G, Van Rompaey V, Ponsaerts P. Transduction Efficiency and Immunogenicity of Viral Vectors for Cochlear Gene Therapy: A Systematic Review of Preclinical Animal Studies. *Frontiers in Cellular Neuroscience* 2021;15.

29. Kawamoto K, Oh SH, Kanzaki S, Brown N, Raphael Y. The functional and structural outcome of inner ear gene transfer via the vestibular and cochlear fluids in mice. *Mol Ther* 2001;4(6):575–85. [PubMed: 11735342]
30. Lee S, Song JJ, Beyer LA, Swiderski DL, Prieskorn DM, Acar M, et al. Combinatorial Atoh1 and Gfi1 induction enhances hair cell regeneration in the adult cochlea. *Sci Rep* 2020;10(1):21397. [PubMed: 33293609]
31. Shu Y, Tao Y, Li W, Shen J, Wang Z, Chen ZY. Adenovirus Vectors Target Several Cell Subtypes of Mammalian Inner Ear In Vivo. *Neural Plast* 2016;2016:9409846. [PubMed: 28116172]
32. Kawamoto K, Yagi M, Stöver T, Kanzaki S, Raphael Y. Hearing and hair cells are protected by adenoviral gene therapy with TGF-beta1 and GDNF. *Mol Ther* 2003;7(4):484–92. [PubMed: 12727111]
33. Yagi M, Kanzaki S, Kawamoto K, Shin B, Shah PP, Magal E, et al. Spiral ganglion neurons are protected from degeneration by GDNF gene therapy. *J Assoc Res Otolaryngol* 2000;1(4):315–25. [PubMed: 11547811]
34. Richter M, Saydaminova K, Yumul R, Krishnan R, Liu J, Nagy EE, et al. In vivo transduction of primitive mobilized hematopoietic stem cells after intravenous injection of integrating adenovirus vectors. *Blood* 2016;128(18):2206–17. [PubMed: 27554082]
35. Bramson JL, Grinshtein N, Meulenbroek RA, Lunde J, Kottachchi D, Lorimer IA, et al. Helper-dependent adenoviral vectors containing modified fiber for improved transduction of developing and mature muscle cells. *Hum Gene Ther* 2004;15(2):179–88. [PubMed: 14975190]
36. Han IC, Burnight ER, Kaalberg EE, Boyce TM, Stone EM, Fingert JH, et al. Chimeric Helper-Dependent Adenoviruses Transduce Retinal Ganglion Cells and Müller Cells in Human Retinal Explants. *J Ocul Pharmacol Ther* 2021;37(10):575–9. [PubMed: 34597181]
37. Kemper C, Leung M, Stephensen CB, Pinkert CA, Liszewski MK, Cattaneo R, et al. Membrane cofactor protein (MCP; CD46) expression in transgenic mice. *Clin Exp Immunol* 2001;124(2):180–9. [PubMed: 11422193]

Highlights:

- HdAd is a versatile viral vector with large carrying capacity that can overcome size limitations of adeno-associated virus vectors.
- HdAd5 transduces multiple cell types within the cochlea including mesenchymal cells, supporting cells and inner hair cells.
- HdAd5 transduction varies by delivery route and transduction of cells within the organ of Corti is achieved by direct delivery in to the scala media.
- HdAd5/35 transduction in the mouse inner ear is CD46 dependent.

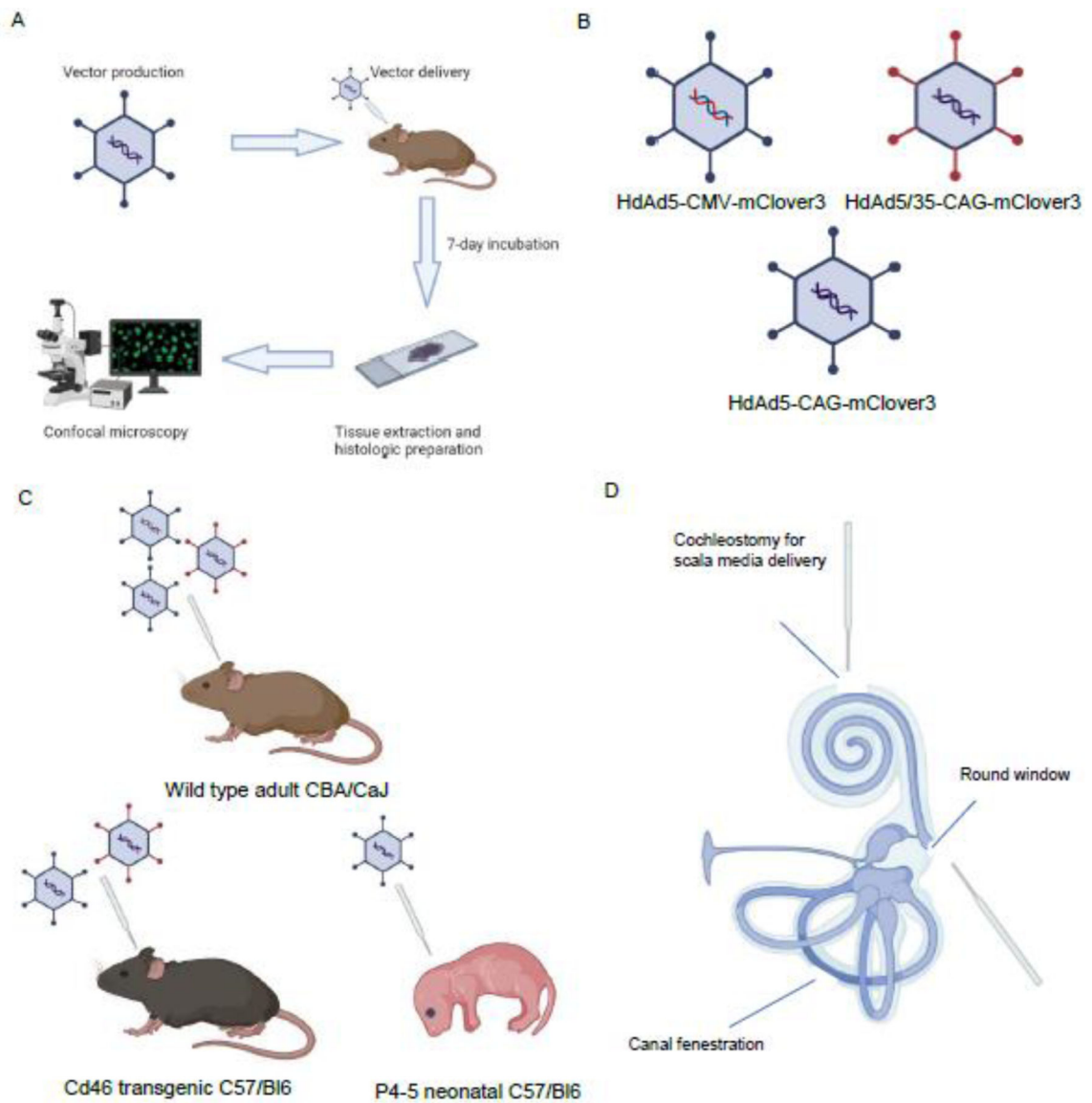


Figure 1: Overview of study methodology.

A: Brief overview of experimental timeline B: Three viral vector constructs carrying fluorescent reported mClover3 were produced. HdAd5 vector constructs expressing mClover3 under the control of both CAG and CMV promoters were produced as well as an HdAd 5/35 construct expressing mClover3 under control of a CAG promoter. C: Three mouse models were used in our experiments. CBA/CaJ wild type adult mouse was injected with all three viral vector constructs. CD46 transgenic mice on a C57/Bl6 background were injected with HdAd5-CAG-mClover3 and HdAd 5/35-CAG-mClover3 constructs. Neonatal C57/Bl6 mice were injected with HdAd 5-CAG-mClover3 viral construct. D: Illustration of approaches used to deliver viral vector. Created with [Biorender.com](https://www.biorender.com)

HdAd5 transduction in adult CBA/CaJ mice by RW+CF approach

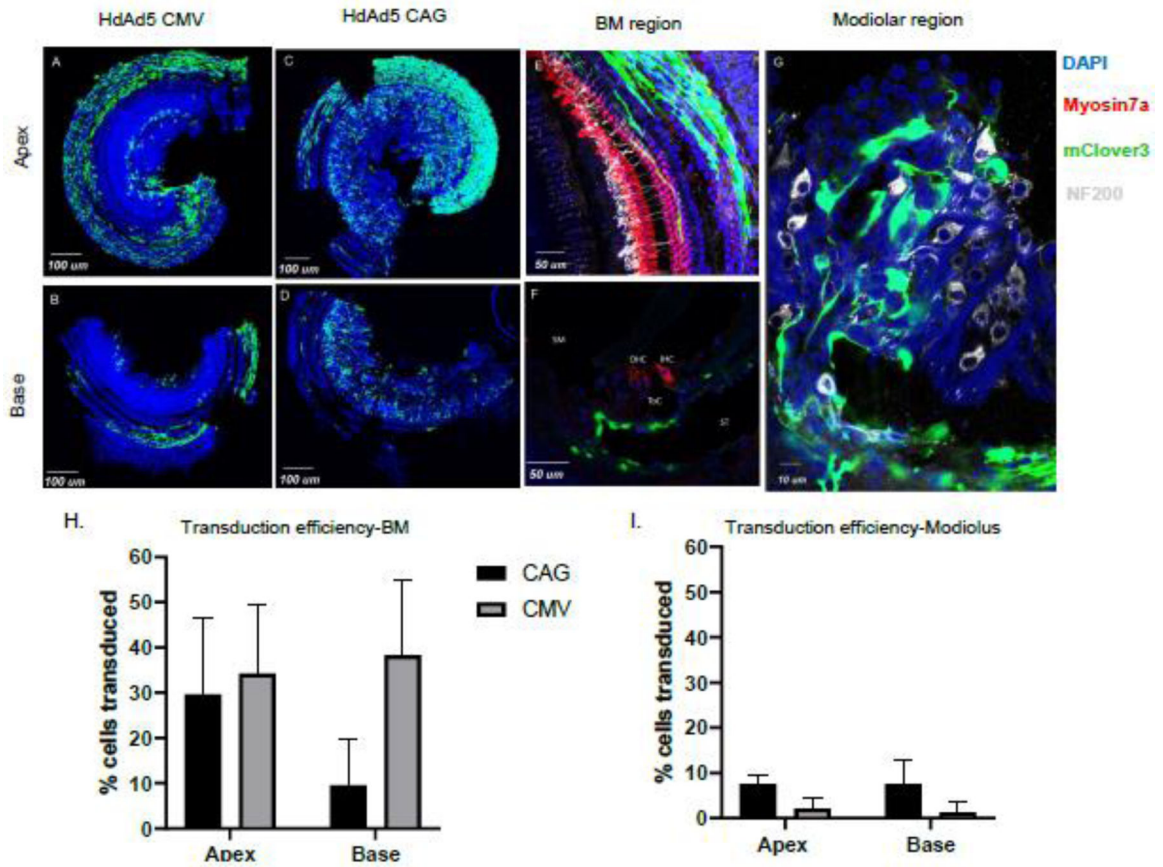


Figure 2: HdAd5 predominantly transduces cells lining the scala tympani and in the modiolar region when injected by RW+CF approach in adult CBA/CaJ mice.

A/B: organ of Corti whole mounts of apical and basal segments from CBA/CaJ mouse injected with HdAd5 under control of CMV promoter (3.44×10^9 viral particles/animal) or HdAd5/35-CAG-mclover3 (1.21×10^9 viral particles/animal). C/D: organ of Corti whole mounts of apical and basal segments from mouse injected with HdAd5 under control of CAG promoter (3.83×10^9 viral particles/animal). E: Apical segment of organ of Corti whole mount illustrating basement membrane region transduction F: Mid-modiolar section of basal segment illustrating basement membrane region transduction. G: Modiolar region from whole mount of basal segment illustrating non-neuronal spiral ganglion transduction. H/I: Comparison of transduction efficiency achieved by HdAd5 under control of CAG vs. CMV promoters in CBA/CaJ mice. BM: basilar membrane region. SM: scala media. ST: scala tympani OHC: outer hair cells. IHC: inner hair cells.

HdAd5 transduction in adult CBA/CaJ mice by SM approach

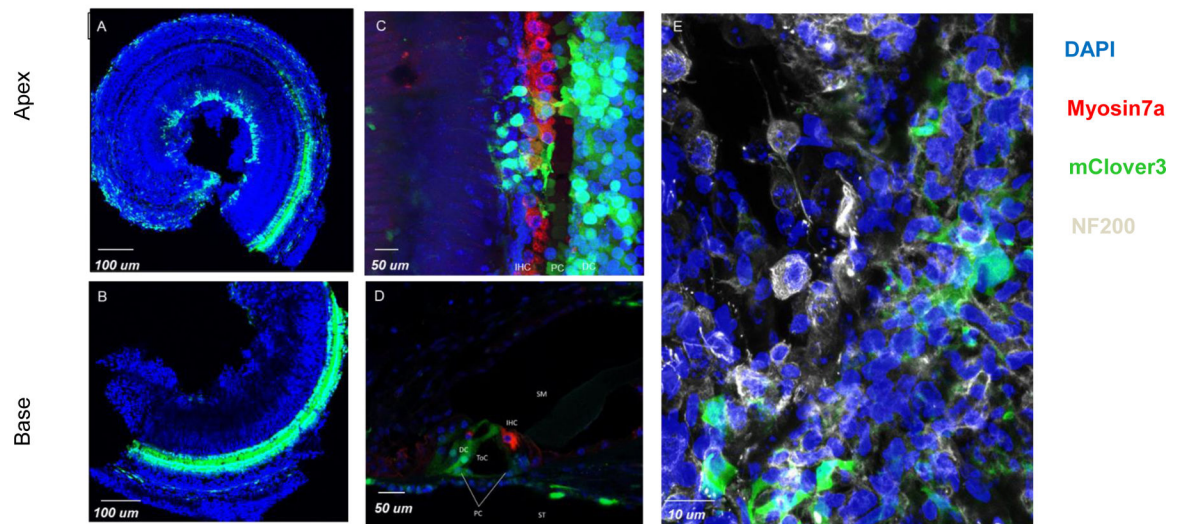


Figure 3: HdAd5 transduces inner hair cells, supporting cells and non-neuronal cells in the spiral ganglion when injected by scala media approach in adult CBA/CaJ mice.

A/B: organ of Corti whole mounts of apical and basal segments from adult CBA mice injected with HdAd5 under control of CMV promoter by scala media approach. C: organ of Corti whole mount of apical segment illustrating inner hair cell and supporting cell transduction. D: Mid-modiolar section of basal segment illustrating supporting cell transduction. E: Modiolar region from whole mount of basal segment illustrating non-neuronal transduction in the spiral ganglion. BM: Basilar membrane region. SM: Scala Media. ST: Scala tympani OHC: outer hair cells. IHC: inner hair cells. PC: Pillar cells. DC: Deiter cells.

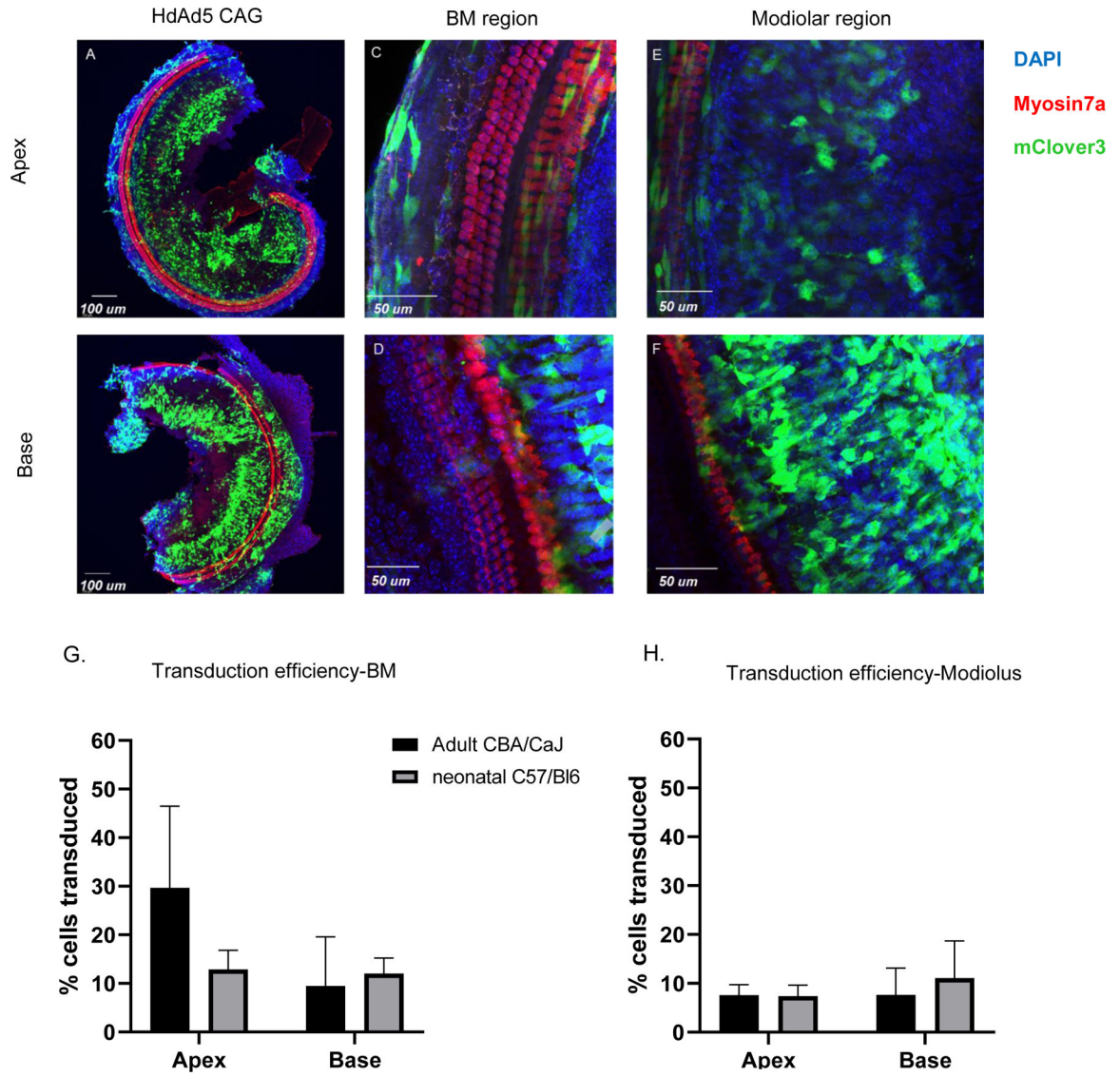


Figure 4: HdAd5 predominantly transduces cells lining the scala tympani and in the modiolar region when injected by RW approach in neonatal C57/Bl6 mice.
 A/B: organ of Corti whole mounts of apical and basal segments from neonatal mice injected with HdAd5 under control of CAG promoter C/D: Apical and basal segments of organ of Corti whole mount illustrating basement membrane region transduction. E/F: Apical and basal segments of organ of Corti whole mount illustrating modiolar region transduction. G/H: Comparison of transduction efficiency achieved by HdAd5 under control of CAG in adult vs. neonatal mice. BM: Basement membrane.

CD46 expression is widespread within the inner ear of CD46 Tg mice

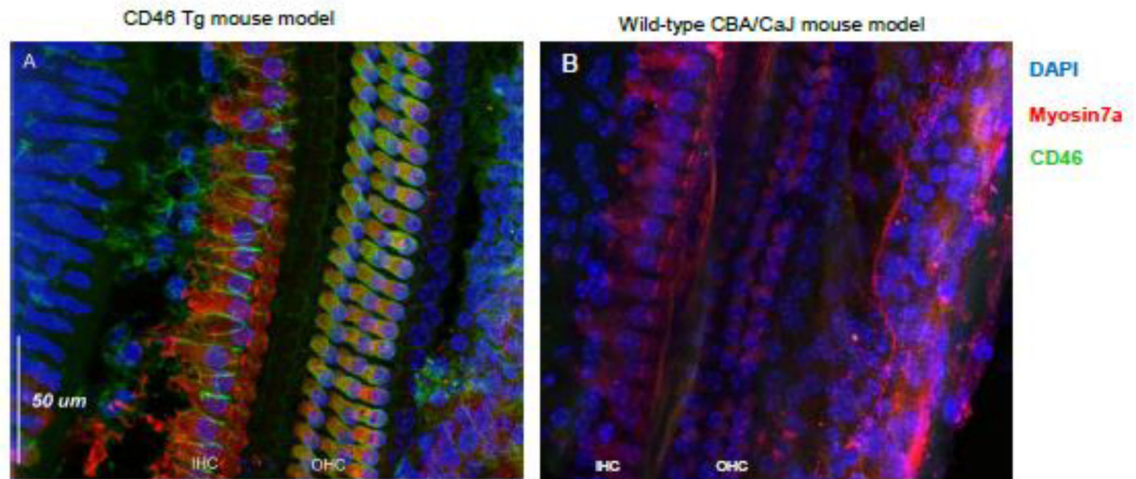


Figure 5: Human CD46 is expressed on multiple cell types in the inner ear of CD46 tg mice. No expression is seen in wild-type controls. A: organ of Corti whole mount illustrating human CD46 expression CD46 Tg mice. CD46 is expressed in green and is seen on the surface of inner and outer hair cells as well as supporting cells. B: CD46 staining of wild-type CBA/CaJ mouse organ of Corti reveals no expression of CD46. IHC: inner hair cells. OHC: Outer hair cells.

HdAd 5/35 transduction in adult CD46 Tg and CBA/CaJ mice

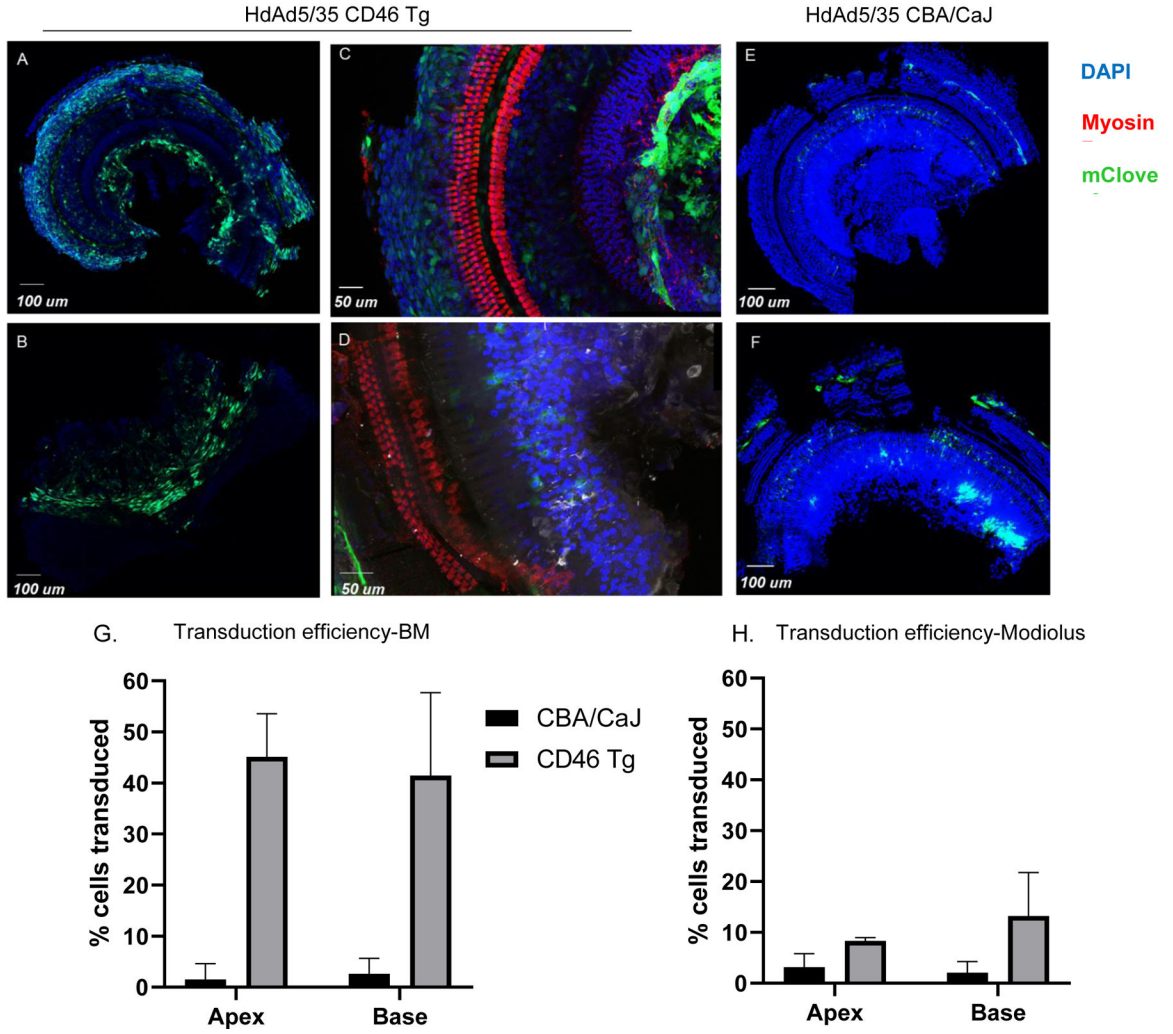


Figure 6: HdAd5/35 transduces cells lining the scala tympani and in the modiolar region when injected by RW+CF approach with higher efficiency in adult CD46 Tg mice. A-D: organ of Corti whole mounts of apical and basal segments from CD46 Tg mouse injected with HdAd5/35 under control of CAG promoter (1.21×10^9 viral particles/ animal). E/F: organ of Corti whole mounts of apical and basal segments from CBA/CaJ mouse injected with HdAd5/35 under control of CAG promoter (1.21×10^9 viral particles/ animal). E: Apical segment of organ of Corti whole mount illustrating basement membrane region transduction. G/H: Comparison of transduction efficiency achieved by HdAd5/35 under control of CAG in CD46 Tg vs. CBA/CaJ mice.